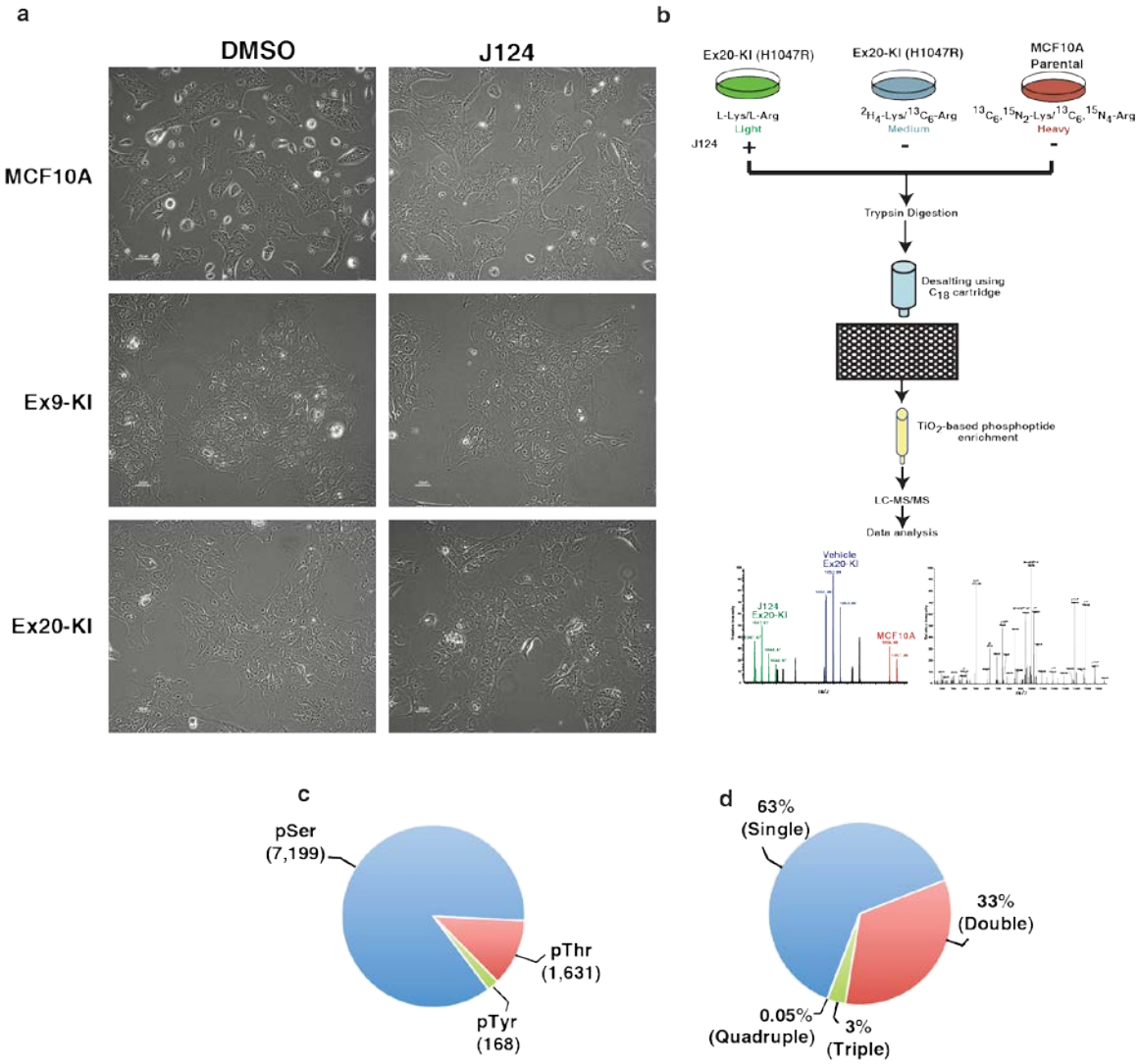

Supplementary Figure 1. Phosphoproteomic analysis of *PIK3CA* mutations. (a) Phase-contrast photomicrographs of MCF10A, Ex9-KI and Ex20-KI cells seeded in DMEM-F12 with 5% horse serum overnight and treated with 0.2 ng ml^{-1} EGF for 3 hours and followed by 30 minutes treatment of 500 ng ml^{-1} J124. Scale bar: 50 µm (b) A schematic depicting the strategy used for quantitative phosphoproteomic profiling of *PIK3CA* EX20 knockin mutant cells. (c) Number of phosphoserine (pSer), phosphothreonine (pThr) and phosphotyrosine (pTyr) sites identified in the study. (d) Distribution of single, double, triple and quadruply phosphorylated peptides identified is indicated.

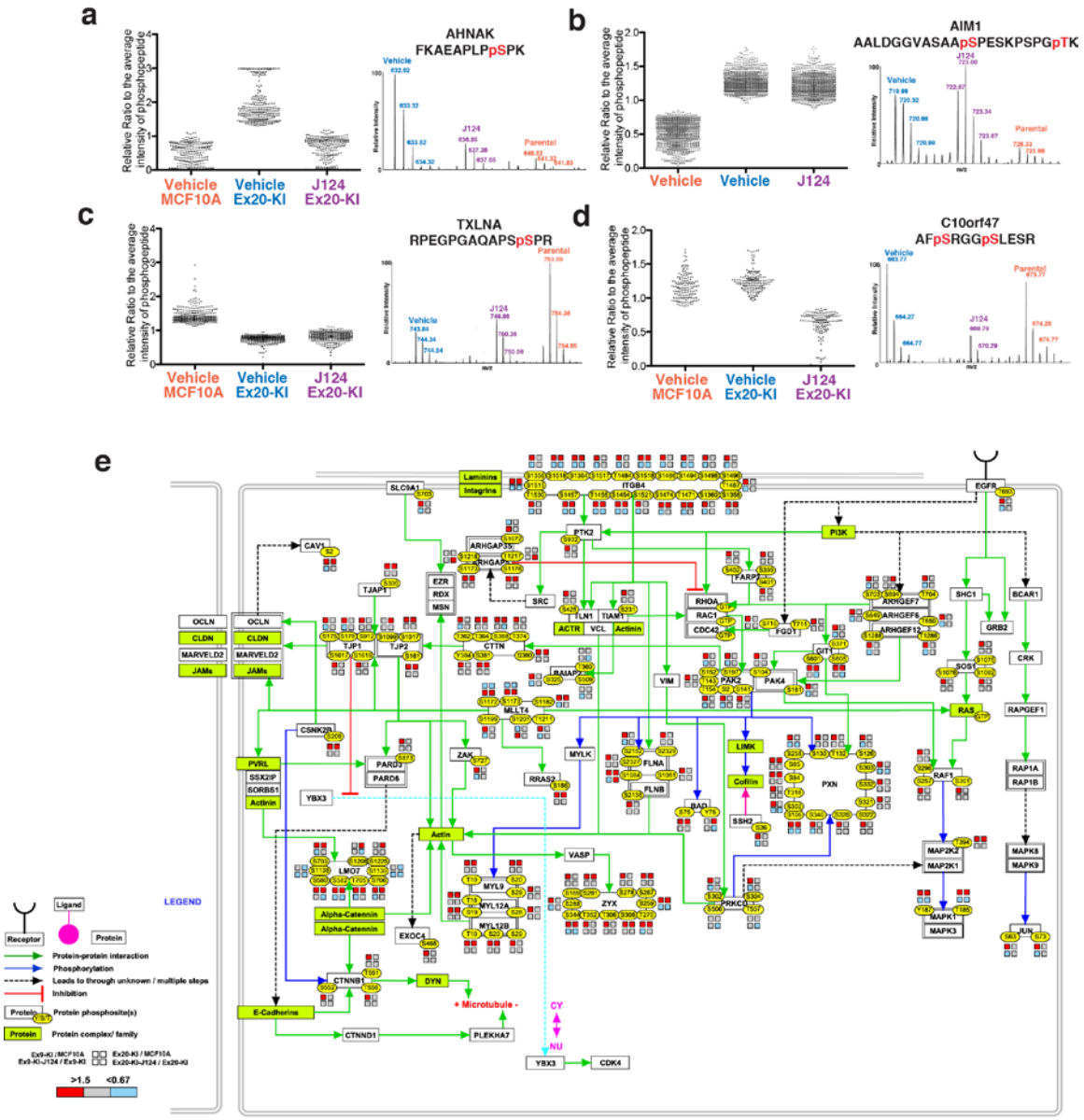

Supplementary Figure 2. Phosphorylation regulation patterns in MCF10A, Ex20-KI and J124-treated Ex20-KI cells. (a-d) Phosphorylation patterns in MCF10A, Ex20-KI and J124-treated Ex20-KI cells. Phosphopeptides with similar phosphorylation profiles were grouped into four major clusters. Representative MS spectra of modulated phosphopeptides corresponding to each regulation pattern type are shown along with the phosphopeptide sequences. (e) The model highlights the literature-curated interaction network of proteins identified in the current study involved in the regulation and assembly of tight junction, adherens junction and focal adhesion represented using

PathVisio (http://www.pathvisio.org/). The protein-protein interaction and the catalysis information for these molecules are extracted from Human Protein Reference Database and Ingenuity pathway database. The phosphosites of proteins that are differentially regulated by the *PIK3CA* mutants and/or the *PIK3CA* inhibitor are distinguished. These phosphoproteins include tight junction assembly proteins such as TJP1, TJP2, and cortactin; proteins in focal adhesion complexes such as ITGB4, PTK2, TLN1, TIAM1, and filamins; adherens junction proteins such as CTNNB1, and LMO7. The map also represents the proteins identified to be involved in the assembly and regulation of the actin cytoskeleton such as myelin light chains, RhoGEFs, PAKs, SSH2, PRKCD, and the components of the RAS/RAF signaling pathway. The details of the nodes and edges specified are indicated in the figure.

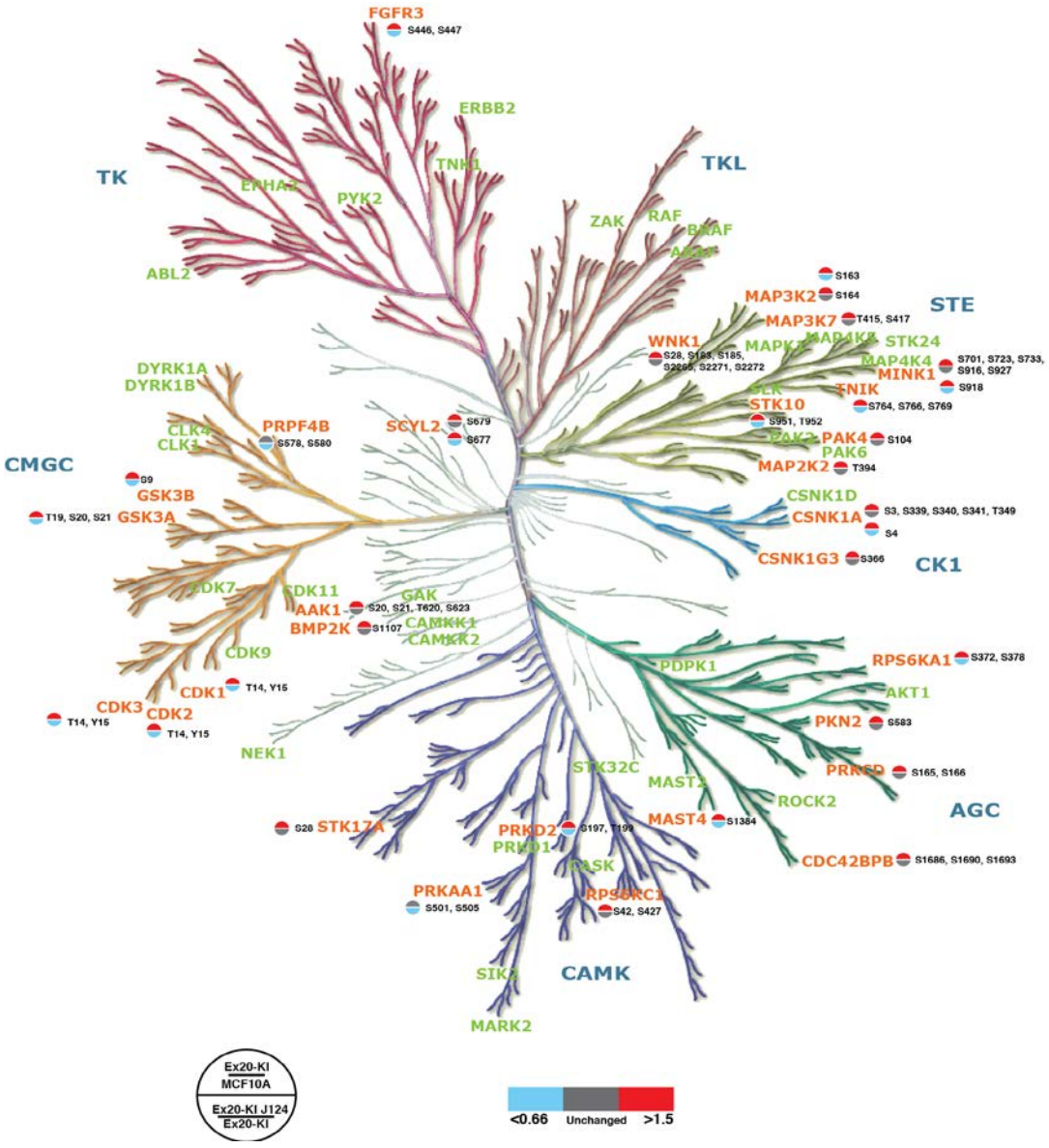

Supplementary Figure 3. Widespread modulation of the kinome observed in *PIK3CA* Ex20-KI cells. A phylogenetic tree (modified from Human Kinome Tree (Manning et al., 2002)) of protein kinases identified in Ex20-KI cells. Hyperphosphorylated kinases are in orange and kinases identified, but not changed in phosphorylation, are in light green. A color-coded site regulation pattern is shown in the form of a circle divided into two parts. Top half represents the fold-change of phosphorylation sites identified in Ex20-KI cells compared to MCF10A, whereas the bottom half represents the fold change ratio between J124-treated Ex20-KI cells compared to untreated ones.

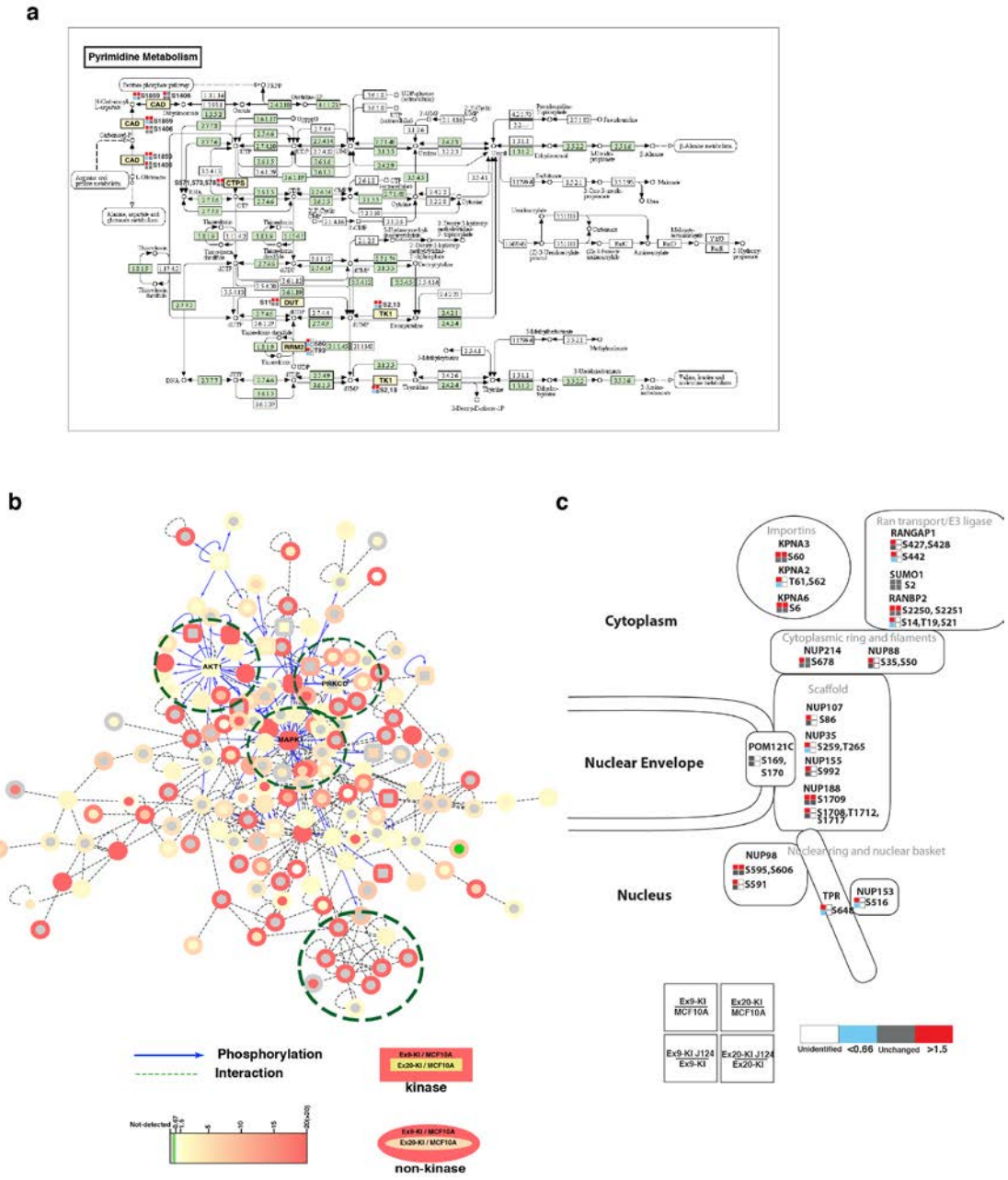

Supplementary Figure 4. Phosphorylation modulated proteins involved in pyrimidine metabolism and nuclear pore complex. (a) Phosphorylation-regulated key enzymes in pyrimidine metabolism pathway modified from KEGG. (b) A network of kinase-substrate and protein-protein interactions within stringently regulated phosphoproteins was generated using Cytoscape. The proteins are color-coded based on the relative abundance of phosphopeptides (Ex9-KI vs. MCF10A cells outer circle and Ex20-KI vs. MCF10A inner circle). (c) Phosphorylation-regulated proteins involved in nuclear pore complex.

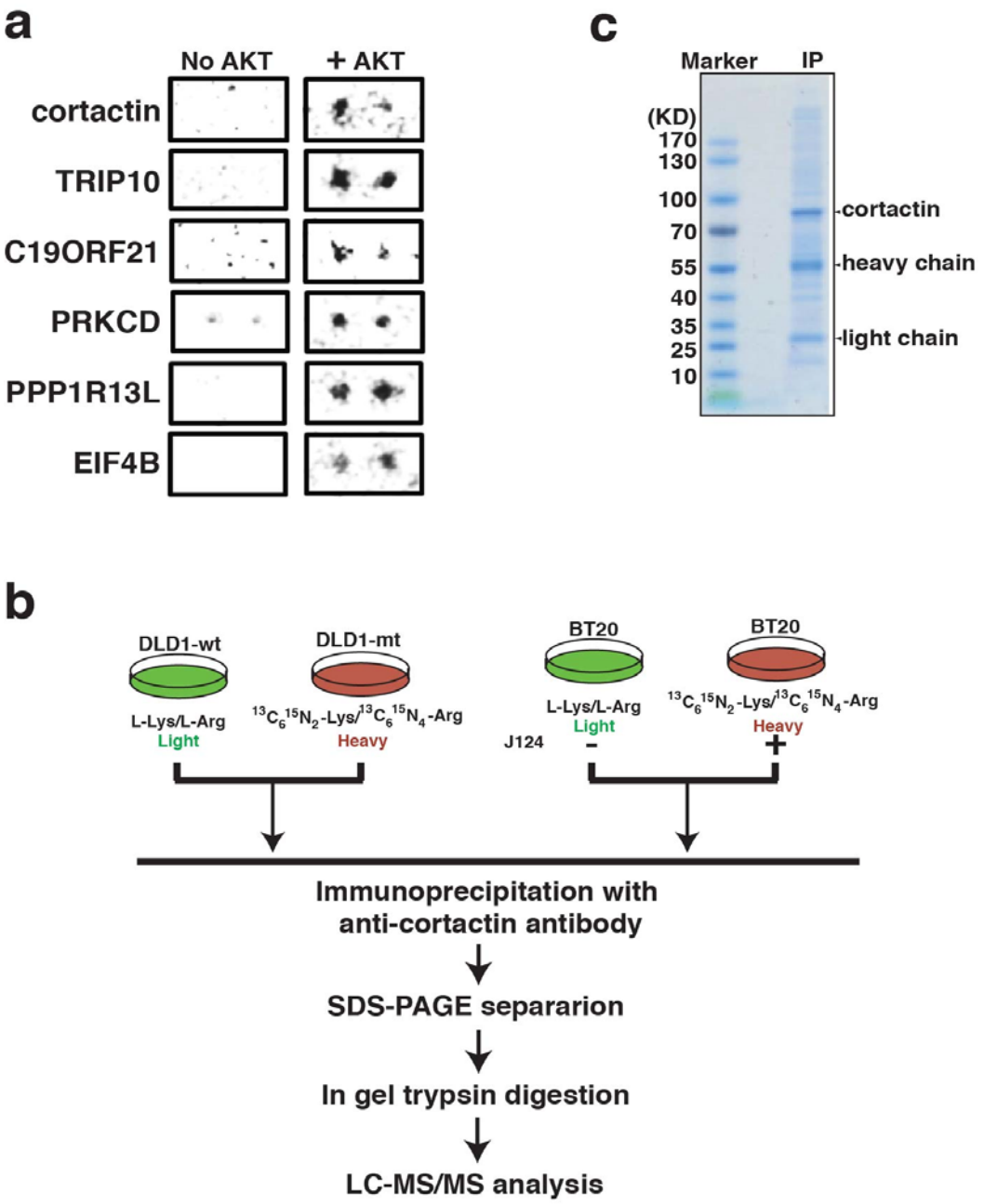

Supplementary Figure 5. Autoradiograph of novel AKT1 substrates identified from protein microarray-based AKT1 substrate assays. Left panel: autoradiographs of the reactions without AKT1; Right panel: autoradiograph of the reactions incubated with AKT1. (b) Phosphoproteomic strategy to validate cortactin phosphorylation sites in DLD1-wt, DLD1-mt and BT20 cells. (c) The panel shows a representative Coomassie blue stained gel from cortactin IP from BT20 cells.

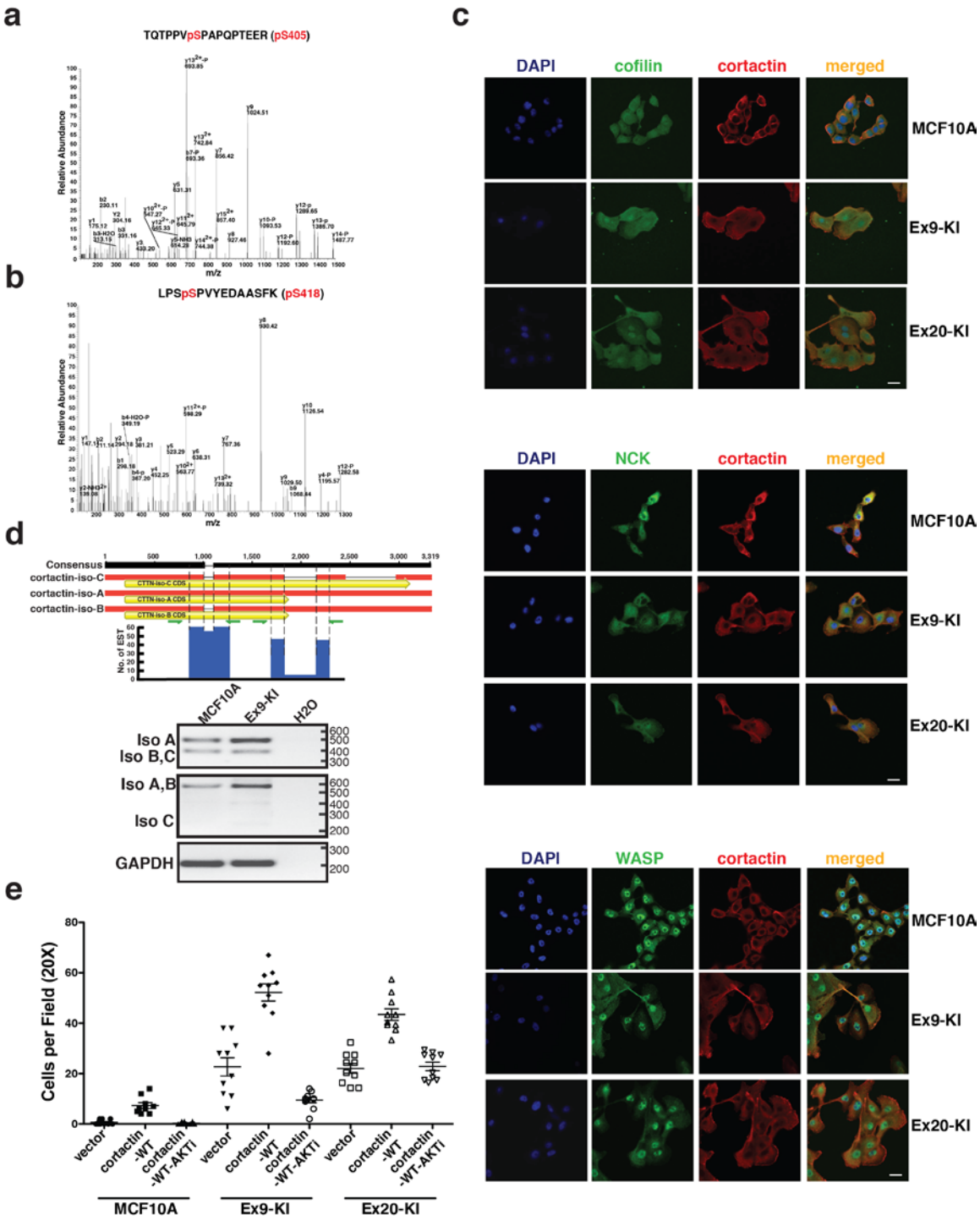

Supplementary Figure 6. Cortactin is a novel substrate of AKT. (a,b) Representative MS/MS spectra of two phosphopeptides identified in AKT-cortactin *in vitro* phosphorylation analysis. (c) Confocal immunofluorescence images of localization pattern of cortactin in red and cofilin (top panel), NCK1 (middle panel) and WASP

(bottom panel) in green in MCF10A, Ex9-KI and Ex20-KI cells. Nuclei were stained with 4,6-diamidino-2-phenylindole (DAPI). Scale bar = 20 μm. (d) Top panel: Alignment of mRNA sequences of three cortactin isoforms. Red bar: mRNA segments, thin black line: gaps, yellow arrow bars: CDS and short green arrows RT-PCR primers. Middle panel: Number of ESTs specifically matched to the alternative splicing sties. Bottom panel: RT-PCR results from MCF10A and Ex9-KI cells. Top panel: RT-PCR results from the upstream pair of primers differentiating isoform A and isoform B and/or C; middle panel: the downstream pair of primers differentiating isoform A and/or B and isoform C. Bottom panel: GAPDH as internal control. (e) Migration/invasion assays for MCF10A, Ex9-KI and Ex20-KI cells overexpressing wild type cortactin (cortactin-wt) treated with vehicle or AKT inhibitor (AKTi). The empty vector retrovirus infected cells served as controls. Data are shown as mean ± s.e.m. Mann-Whitney test was carried out to determine the statistical significance. These experiments were repeated at least twice.

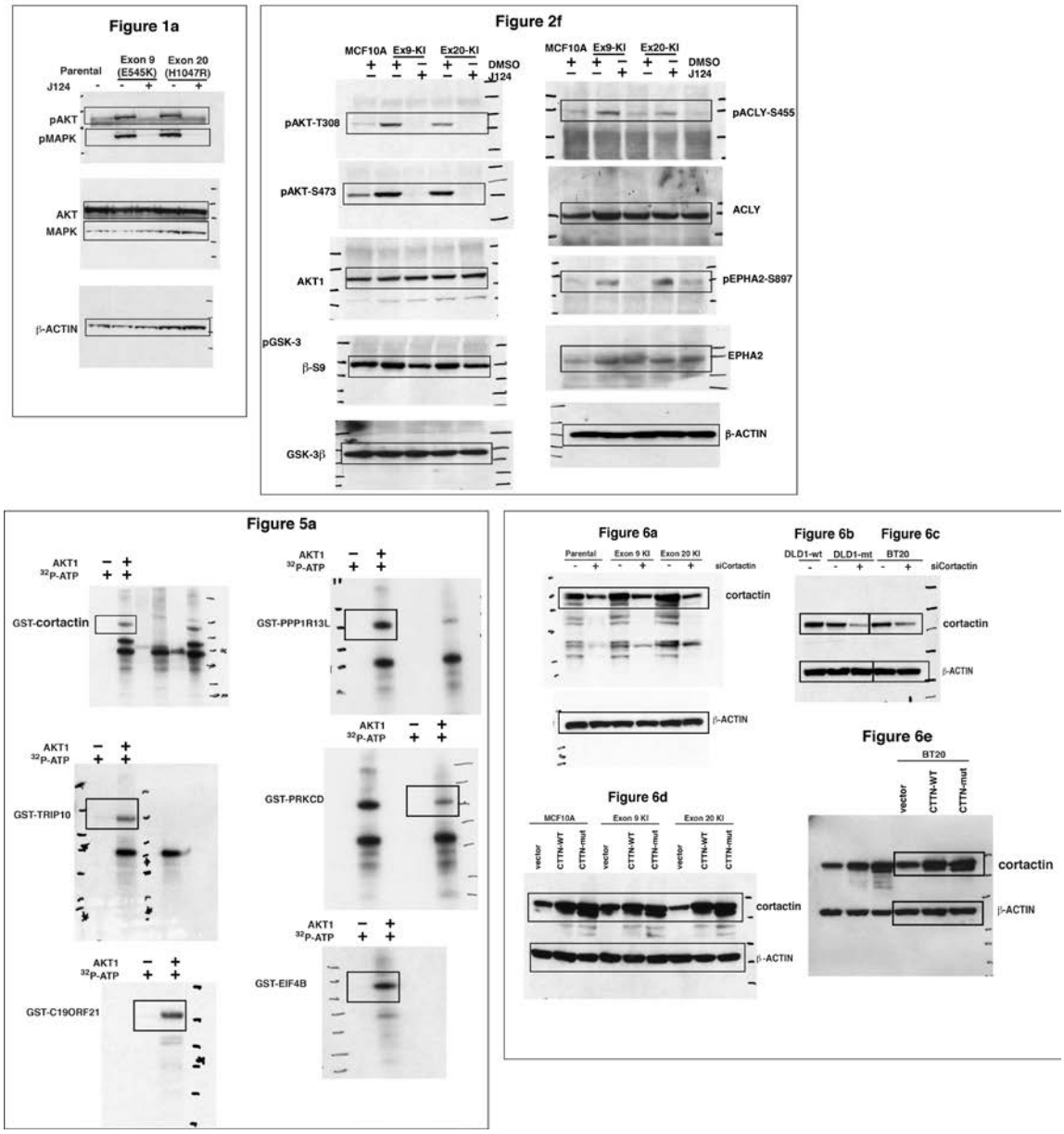

Supplementary Figure 7. Full scans of the corresponding figures where the cropped images (marked as boxes) appear are indicated.